Dynamic Nature of Nonculprit Coronary Artery Lesion Morphology in STEMI

A Serial IVUS Analysis From the HORIZONS-AMI Trial

Zhijing Zhao, MD,* Bernhard Witzenbichler, MD,† Gary S. Mintz, MD,‡
Markus Jaster, MD,† So-Yeon Choi, MD, PhD,* Xiaofan Wu, MD, PhD,* Yong He, MD,*
M. Pauliina Margolis, MD, PhD,§ Ovidiu Dressler, MD,* Ecaterina Cristea, MD,‖
Helen Parise, ScD,* Roxana Mehran, MD,¶ Gregg W. Stone, MD,* Akiko Maehara, MD*

New York, New York; Berlin, Germany; and Rancho Cordova, California

OBJECTIVES The authors sought to report the temporal stability of an untreated, nonculprit lesion phenotype in patients presenting with ST-segment elevation myocardial infarction (STEMI).

BACKGROUND The temporal stability of the untreated, nonculprit lesion phenotype has been studied using intravascular ultrasound-virtual histology (IVUS) in patients with stable ischemic heart disease, but not in STEMI patients.

METHODS As part of a formal substudy of the HORIZONS-AMI (Harmonizing Outcomes With Revascularization and Stents in Acute Myocardial Infarction) trial, baseline and 13-month follow-up IVUS was performed in 99 untreated nonculprit lesions in 63 STEMI patients. Lesions were classified as pathological intimal thickening (PIT), IVUS–derived thin-cap fibroatheroma (TCFA), thick-cap fibroatheroma (ThCFA), fibrotic plaque, or fibrocalcific plaque.

RESULTS The frequency of TCFA increased from 41% at baseline to 54% at follow-up, whereas ThCFAs decreased from 41% to 34% and PIT decreased from 16% to 8%. Among the 41 lesions classified at baseline as TCFA, at follow-up, 32 (78%) were still classified as TCFA, whereas 9 (22%) were classified as ThCFAs or fibrotic plaques. An additional 21 lesions at follow-up were newly classified as TCFA, developing from either PIT or ThCFA. TCFA at baseline that evolved into non-TCFAs trended toward a more distal location than TCFA that did not change (p = 0.12). In lesions classified as TCFA, the minimum lumen area (MLA) decreased from 8.1 (interquartile range [IQR]: 7.4 to 8.8) mm^2 at baseline to 7.8 (IQR: 7.2 to 8.4) mm^2 at follow-up, p < 0.05; this was associated with an increase in percent necrotic core at the MLA site (14% [IQR: 12 to 16] to 19% [IQR: 17 to 22], p < 0.0001) and over the entire length of the lesion (14% [IQR: 12 to 16] to 18% [IQR: 17 to 20], p < 0.0001).

CONCLUSIONS Untreated nonculprit lesions in STEMI patients frequently have TCFA morphology that does not change during 13-month follow-up and is accompanied by a decrease in MLA and an increase in necrotic core. (Harmonizing Outcomes With Revascularization and Stents in Acute Myocardial Infarction [HORIZONS-AMI]; NCT00433966) (J Am Coll Cardiol Img 2013;6:86–95) © 2013 by the American College of Cardiology Foundation

utopsy data suggest that rupture of an atheromatous plaque with superimposed thrombosis is the cause of most acute coronary syndromes (ACS) and sudden cardiac death (1–3). A thin-cap fibroatheroma (TCFA) with a large lipid-rich necrotic core (NC) is particularly prone to rupture and result in coronary artery thrombotic occlusion (4–7). Furthermore, 3-vessel imaging studies in patients with ACS have shown that the incidence of secondary plaque rupture in nonculprit lesions is fairly common (8). Intravascular ultrasound-virtual histology (IVUS) provides quantitative and qualitative information about plaque composition and lesion phenotype, including plaques prone to cause events (9–12), and may therefore be useful to assess serial plaque composition evolution. A previous IVUS study in patients, mostly with stable ischemic heart disease, demonstrated that the IVUS lesion phenotype can evolve and, specifically, that virtual histology–derived thin-cap fibroatheromas (TCFA) can develop and/or heal within 1 year (13). No such studies have been performed in patients with ACS. In the present study, therefore, we used serial (baseline and follow-up) IVUS to assess the dynamic nature of nonculprit coronary artery lesion morphology in patients with ST-segment elevation myocardial infarction (STEMI), in particular to evaluate the development and evolution of TCFA.

METHODS

Study population. HORIZONS-AMI (Harmonizing Outcomes With Revascularization and Stents in Acute Myocardial Infarction) was a prospective, open-label, multicenter, dual-arm, 2×2 factorial randomized trial in patients with STEMI. The 2 randomization arms consisted of: 1) the direct thrombin inhibitor bivalirudin alone versus heparin plus a glycoprotein IIb/IIIa inhibitor (1:1 randomization); and 2) TAXUS EXPRESS paclitaxel-eluting stents versus otherwise equivalent EXPRESS bare-mental stents (3:1 randomization) (Boston Scientific, Natick, Massachusetts). The present study cohort consists of 63 patients (99 lesions) with serial IVUS examinations of at least 1 untreated nonculprit lesion in a native coronary artery

at baseline and at follow-up that were studied at Charitė University Medicine Berlin (Campus Benjamin Franklin, Berlin, Germany) where the ethics committee approved the protocol, and written informed consent was obtained from all patients.

Clinical follow-up. Clinical follow-up was performed at 30 days, 6 months, 1 year, 2 years, and 3 years. Routine angiographic (with or without IVUS) follow-up was performed at 13 months or earlier if a clinical event occurred. Pre-specified endpoints included ischemia-driven revascularization and the composite of major adverse cardiac events (death, reinfarction, stroke, or stent thrombosis). An independent clinical events committee (Cardiovascular Research Foundation [CRF], New York, New York) that was masked to treatment assignment adjudicated all adverse events from original source documents and procedural angiograms.

IVUS image acquisition. After intracoronary nitroglycerin, a phased-array, 20-MHz, 3.2-F IVUS catheter (Eagle Eye, Volcano Corporation, Rancho Cordova, California) was placed into the distal coronary artery and pulled back to the aorto-ostial junction using an R-100 motorized catheter pullback device (Volcano Corporation) at a speed of 0.5 mm/s. During pull back, grayscale IVUS was recorded, raw radiofrequency data were captured at the top of the R-wave, and reconstruction of the color-coded map by an IVUS data recorder was performed (In-Vision Gold, Volcano Corporation). The grayscale IVUS and captured radiofrequency data were written onto a CD-R or DVD-R and sent to an independent IVUS core laboratory (CRF) for quantitative and qualitative analyses.

Grayscale and IVUS analyses. Off-line grayscale and IVUS analyses were performed using: 1) QCU-CMS (Medis, Leiden, the Netherlands) for contouring; 2) pcVH 2.1 software (Volcano Corporation) for contouring and data output; and 3) proprietary qVH software (qVH 2.5, developed and

validated at CRF) for qualitative segmental assessment and quantitative data output. Corresponding baseline and follow-up images were identified by the distance from 2 fiduciary landmarks such as side branches and stent edges. Quantitative grayscale IVUS measurements of lumen, external elastic membrane (EEM), and plaque and media (defined as EEM minus lumen) cross-sectional area (CSA) and plaque burden (defined as plaque and media divided by EEM) were performed for every recorded frame. IVUS analysis was also performed for every recorded frame. Volumes were calculated using Simpson's rule and normalized for analysis length. The 4 IVUS plaque components were color-coded as white (dense calcium [DC]), red (NC), light green (fibrofatty [FF]), and dark green (fibrotic tissue [FT]), and reported as CSA and percentage of total plaque CSA and volume. Volumetric grayscale and IVUS analyses were performed only for lesions in which motorized pull back was consistent and reliable.

Definition of lesion types. Lesions were classified by 2 experienced, independent observers (Z.Z. and A.M.) on the basis of plaque composition. Interobserver variability was good ($\kappa = 0.87$), and disagreements were resolved by consensus discussion. Fibroatheromas (TCFA and thick-cap fibroatheroma [ThCFA]) contained >10% confluent NC in at least 3 consecutive frames. Because the window size currently applied for the selection of the region of interest and the eventual tissue map or IVUS image reconstruction using this system and catheter is approximately 246 μm in the radial direction, it was not possible to detect fibrous cap thickness <65 μm (the typical pathological definition of a thin fibrous cap) (9). Therefore, TCFA was defined as a fibroatheroma without virtual histology evidence of a fibrous cap, with >30° NC abutting the lumen in at least 3 consecutive frames (12,14). ThCFA was defined as a fibroatheroma with a definable fibrous cap. Fibrotic plaque had mainly FT with <10% confluent NC, <15% FF tissue, and <10% confluent DC. Fibrocalcific plaque had mainly FT with >10% confluent DC, but <10% confluent NC. All other plaques were classified as pathological intimal thickening (PIT), which was mainly a mixture of FT and FF (>15%) with <10% confluent NC and <10% confluent DC. Fibroatheromas were considered multiple and distinct if they were separated by at least 3 consecutive image slices containing a different fibroatheroma subtype (TCFA and/or ThCFA) or a nonfibroatheroma phenotype.

IVUS phenotypes and their evolution were assessed at 2 levels: lesion level and fibroatheroma level. For lesion-level IVUS classification, the entire lesion was evaluated. We identified untreated, nonculprit lesions as having a plaque burden ≥40% in at least 3 consecutive frames (≥1.5 mm in length) and >5 mm from the stent edge. Lesions were considered separate if there was a ≥5-mm-long segment with <40% plaque burden between them. A lesion could contain more than 1 fibroatheroma. Fibroatheromas were considered multiple and distinct if they were separated by at least 3 consecutive frames containing a different lesion phenotype (14). In lesions that contained more than 1 fibroatheroma subtype, the following hierarchy was used: a TCFA took precedence over ThCFA, and any fibroatheroma took precedence over any nonfibroatheroma. If there was no fibroatheroma in the entire lesion, the virtual histology classification at the minimum lumen area (MLA) site was evaluated and defined as fibrotic plaque, fibrocalcific plaque, or PIT. Because a lesion could contain more than 1 fibroatheroma, the evolution of each fibroatheroma within a lesion was also assessed.

Table 1. Baseline Patient Clinical Characteristics (N = 63)

First randomization (to bivalirudin)	33 (52.4%)
Second randomization (to paclitaxel-eluting stent)	51 (81.0%)
Age, yrs	62.7 [52.1–69.2]
Male	53 (84.1%)
Diabetes	12 (19.0%)
Hyperlipidemia	29 (46.0%)
Hypertension	39 (61.9%)
Current smoker	37 (58.7%)
Prior myocardial infarction	2 (3.2%)
Prior percutaneous coronary intervention	4 (6.3%)
Prior coronary artery bypass grafting	3 (4.8%)
Time from symptom onset to first balloon inflation (hours)	4.1 [3.1–8.1]
Killip class 1	62 (98.4%)
Renal insufficiency*	1 (1.6%)
Ejection fraction, %	65.4 [54.9–68.0]
Body mass index	27.0 [24.5–29.3]
Medications at discharge	
Statin	62 (98.4%)
Any thienopyridine	63 (100%)
Aspirin	63 (98.4%)
Medications at 1 year	
Any thienopyridine	54 (85.7%)
Aspirin	62 (98.4%)

Values are n (%) or median [interquartile range]. *Renal insufficiency was defined as a creatinine clearance of <60 ml/min as calculated with the use of the Cockcroft-Gault equation.

Table 2. Changes in Quantitative Grayscale and IVUS Findings Between Baseline and Follow-Up

	Baseline	Follow-Up	p Value
Lesion length, mm	9.9 [8.6–11.2]	9.8 [8.4–11.0]	0.69
Minimum lumen CSA, mm^2	8.1 [7.4–8.8]	7.8 [7.2–8.4]	0.01
Mean lumen CSA, mm^3/mm	9.9 [9.2–10.6]	9.4 [8.8–10.1]	<0.0001
Mean EEM CSA, mm^3/mm	19.8 [18.3–21.3]	19.0 [17.6–20.4]	<0.0001
Mean plaque+media CSA, mm^3/mm	9.9 [9.0–10.8]	9.6 [8.7–10.5]	0.03
Plaque burden, %	49 [48–51]	50 [49–51]	0.34
NC at MLA site, %	14 [12–16]	19 [17–22]	<0.0001
NC at maximum NC site, %	22 [20–24]	27 [25–29]	<0.0001
NC volume, mm^3	8.1 [6.3–9.9]	10.3 [8.2–12.5]	0.003
Mean NC CSA, mm^3/mm	0.8 [0.7–1.0]	1.1 [0.9–1.3]	<0.0001
NC volume, %	14 [12–16]	18 [17–20]	<0.0001
Dense calcium volume, %	6 [5–7]	10 [9–11]	<0.0001
Fibrous tissue volume, %	59 [58–61]	58 [56–60]	0.04
Fibrofatty volume, %	21 [19–23]	14 [12–16]	<0.0001

Values are median [interquartile range].
CSA = cross sectional area; EEM = external elastic membrane; IVUS = intravascular ultrasound-virtual histology; MLA = minimum lumen area; NC = necrotic core.

Statistical analysis. Statistical analysis was performed using SAS software, version 9.1 (SAS Institute, Cary, North Carolina). Categorical variables are presented as frequencies and were compared with the chi-square or Fisher exact test. Continuous variables were presented as medians and interquartile ranges, and were compared using the Wilcoxon signed rank test. For lesion- and fibroatheroma-level data, a model with a generalized estimating equation approach was used to compensate for any potential cluster effect of multiple fibroatheromas or lesions in the same patient using an exchangeable working correlation structure; data were presented as least square means with 95% confidential interval (15). A p value <0.05 was considered statistically significant.

RESULTS

Patient and lesion characteristics. Overall, 99 nonculprit, untreated lesions in 73 target vessels in 63
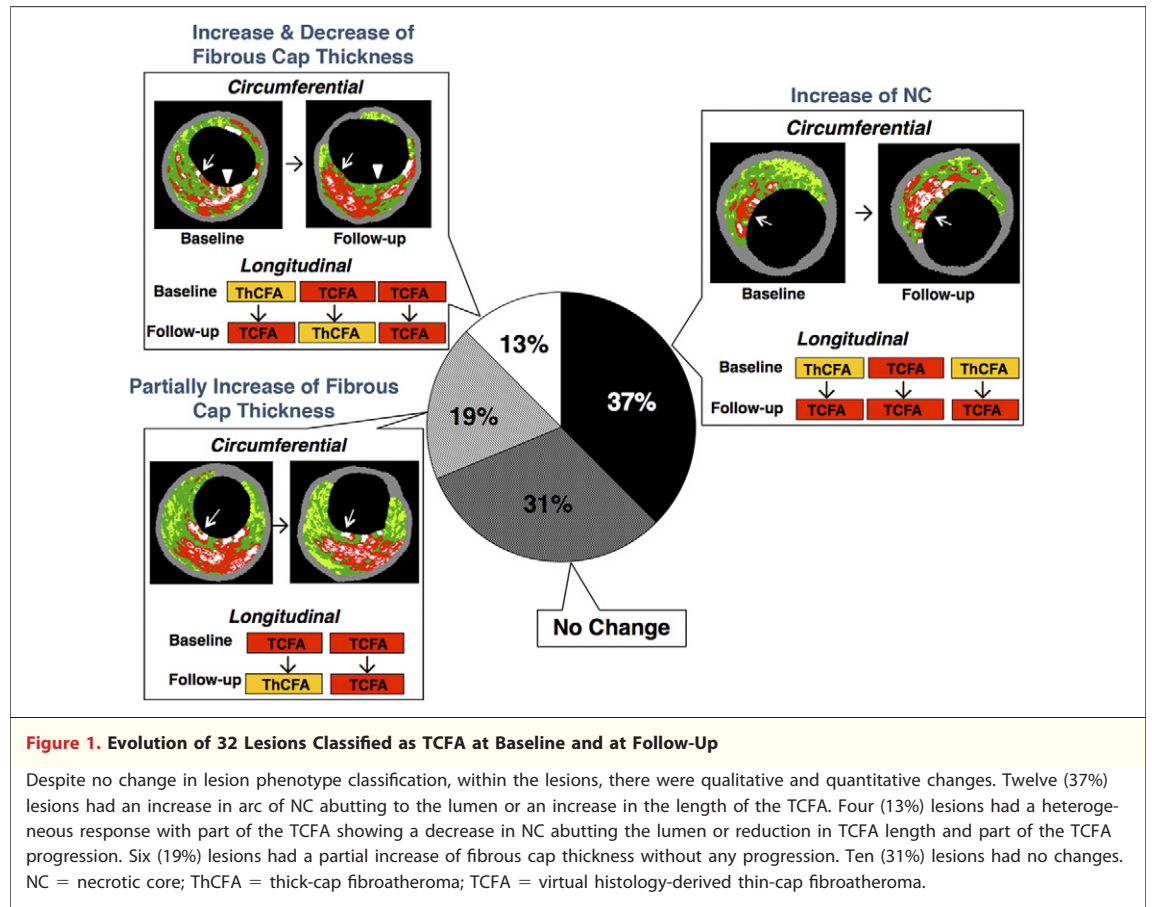
patients were identified and analyzed by grayscale and IVUS at baseline and follow-up. A total of 59 nonculprit lesions were located in the right coronary artery, 19 nonculprit lesions were located in the left anterior descending coronary artery, 9 nonculprit lesions were located in the left circumflex coronary artery, and 12 nonculprit lesions were located in the left main coronary artery. There were 3 predominant IVUS phenotypes at baseline: TCFA (n = 41), ThCFA (n = 41), or PIT (n = 16), whereas 1 additional lesion was classified as fibrocalcific. At follow-up, there were 3 new lesions; 1 was a ThCFA and 2 were PITs.

Baseline clinical characteristics are listed in Table 1. From the baseline to follow-up imaging study, the MLA decreased significantly (from 8.1 [7.4, 8.8] mm^2 to 7.8 [7.2, 8.4] mm^2, p = 0.01); this was associated with an increase in the percent NC, whether assessed at the MLA site (14% [12, 16] to 19% [17, 22], p < 0.0001), over the entire length of

Table 3. Evolution of the Lesion-Level IVUS Phenotype

	Baseline	Follow-Up				
		TCFA	ThCFA	PIT	Fibrotic	Fibrocalcific
TCFA	41 (41%)	32	7	0	2	0
ThCFA	41 (41%)	18	20	2	1	0
PIT	16 (16%)	3	7	6	0	0
Fibrocalcific	1 (1%)	0	0	0	0	1
Total	99	53 (54%)	34 (34%)	8 (8%)	3 (3%)	1 (1%)

Values are n or n (%).
IVUS = intravascular ultrasound-virtual histology; PIT = pathological intimal thickening; ThCFA = thick-cap fibroatheroma; TCFA = virtual histology–derived thin-cap fibroatheroma.

Figure 1. Evolution of 32 Lesions Classified as TCFA at Baseline and at Follow-Up

Despite no change in lesion phenotype classification, within the lesions, there were qualitative and quantitative changes. Twelve (37%) lesions had an increase in arc of NC abutting to the lumen or an increase in the length of the TCFA. Four (13%) lesions had a heterogeneous response with part of the TCFA showing a decrease in NC abutting the lumen or reduction in TCFA length and part of the TCFA progression. Six (19%) lesions had a partial increase of fibrous cap thickness without any progression. Ten (31%) lesions had no changes. NC = necrotic core; ThCFA = thick-cap fibroatheroma; TCFA = virtual histology-derived thin-cap fibroatheroma.

the lesion (14% [12, 16] to 18% [17, 20], p < 0.0001), or at the maximum NC site (22% [20, 24] to 27% [25, 29], p < 0.0001) (Table 2). The change of NC volume was negatively correlated to the change of fibrofatty plaque volume (R = −0.783, p < 0.0001) The frequency of lesions that were classified as TCFA increased from 41% at baseline to 54% at 13-month follow-up, whereas the proportion of ThCFAs and PIT lesions decreased from 41% to 34% and from 16% to 8%, respectively (Table 3). Among the TCFA lesions, 12.5% (5 of 40) of lesions at baseline and 7.8% (4 of 51) of lesions at follow-up had an MLA ≤ 4 mm^2; and 7.5% (3 of 40) of lesions at baseline and 13.7% of lesions (7 of 51) at follow-up had a plaque burden of >70% at the MLA site.

Evolution of lesion-level IVUS phenotype. The temporal progression of nonculprit lesion-level IVUS phenotype is shown in Table 3. At baseline, 41 lesions were classified as TCFA. At follow-up, 32 lesions (78%) were still classified as TCFA, whereas 9 lesions (22%) evolved into ThCFAs or fibrous plaques. An additional 21 lesions were newly classified as TCFA at 13-month follow-up, developing

from either PIT (n = 3, 19% of baseline PITs) or ThCFA (n = 18, 44% of baseline ThCFAs) phenotypes. Among the 32 TCFA that did not change their overall phenotypical classification during follow-up, 37% had an evolution in appearance suggesting an increase in instability: 1) progression (n = 12, 37%), an increase in arc or length of NC abutting to the lumen (implying an increase in the size of the thin cap of the fibroatheroma), or an increase in the length of the TCFA; or 2) decrease and increase of fibrous cap thickness (n = 4, 13%), a heterogeneous response such that part of the TCFA had a decrease in NC abutting the lumen (increase of fibrous cap thickness) or a reduction in TCFA length, while part of the TCFA had a decrease in fibrous cap thickness. Conversely, there was a partial increase of the fibrous cap thickness without any progression in 6 TCFA (19%) and no change in 10 TCFA (31%). This is summarized in Figure 1.

At baseline, there were 41 nonculprit lesions that were classified as ThCFAs. At follow-up, 18 of these ThCFAs evolved into TCFA (Fig. 2) with 2 different patterns: 1) new TCFA within the lesion,
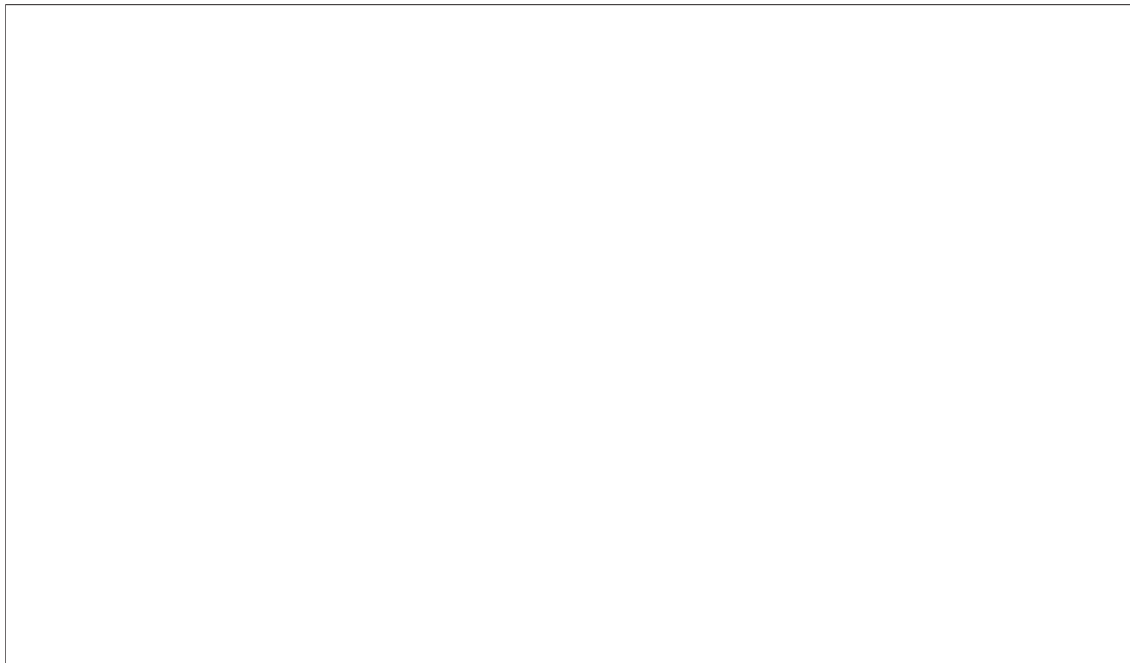
Figure 2. New TCFA at Follow-Up

At follow-up, there were 18 new TCFA. Among them, 7 (39%) lesions had a new TCFA in addition to the baseline ThCFA that did not change. Another 5 (28%) TCFA evolved from a ThCFA with disappearance of the fibrous cap at the site of the baseline ThCFA. In 6 (33%) lesions, there was a new TCFA at a site that previously did not have any fibroatheroma (e.g., PIT that evolved into a TCFA).
PIT = pathologic intimal thickening; other abbreviations as in Figure 1.

either circumferentially (n = 7, 39%) or longitudinally (n = 6, 33%), but at a site unrelated to the baseline ThCFA; or 2) disappearance of fibrous cap at the site of the baseline ThCFA, converting the lesion into a TCFA (n = 5, 28%). Conversely, 20 (49%) baseline ThCFAs were still classified as ThCFA at follow-up, and 3 (7%) evolved into other stable phenotypes.

At baseline there were 16 lesions that were classified as PIT. Of these lesions, 3 (19%) evolved into a TCFA, 76 (43%) evolved into a ThCFA, and 6 (38%) were still classified as a PIT at follow-up.

TCFA distribution at the fibroatheroma level. As shown in Figure 3, approximately 50% of TCFA were located in the proximal 20 mm of the coronary artery both at baseline and at follow-up. Using the distance from the coronary ostium to the maximum NC site, TCFA that healed during follow-up tended to be more distally located than those that did not change (36.2 [24.2, 48.2] mm vs. 25.7 [18.9, 32.6] mm, p = 0.12). The distance between newly developed TCFA at follow-up compared with persistent TCFA from baseline was not significantly different: 27.8 [18.9, 36.8] mm versus 24.7 [17.7, 31.7] mm, p = 0.50.

IVUS findings of patients with late clinical events. During 3 years of follow-up, 4 unplanned revascularizations were required for progressive or unstable angina arising from these 99 nonculprit lesions. In 2 cases, the phenotypes progressed from ThCFAs to TCFA at the time of event; in 1 case, the phenotype progressed from PIT to ThCFA; and 1 case was a TCFA both at baseline and at the time of the event. The grayscale and IVUS findings in these 4 lesions are shown in Table 4.

DISCUSSION

This is the first report, to our knowledge, in which serial (baseline and follow-up) IVUS was used to assess the dynamic nature of nonculprit coronary artery lesion morphology in patients presenting with STEMI. The major findings of our analysis are: 1) more than 82% of untreated, nonculprit lesions in patients with STEMI were fibroatheromas at baseline (half of which were TCFAs), with the majority demonstrating a lack of healing and/or an increase in unstable phenotype during 13 months of follow-up; and 2) fibroatheromas that became more stable in appearance over time tended to be located more distally, whereas fibroatheromas
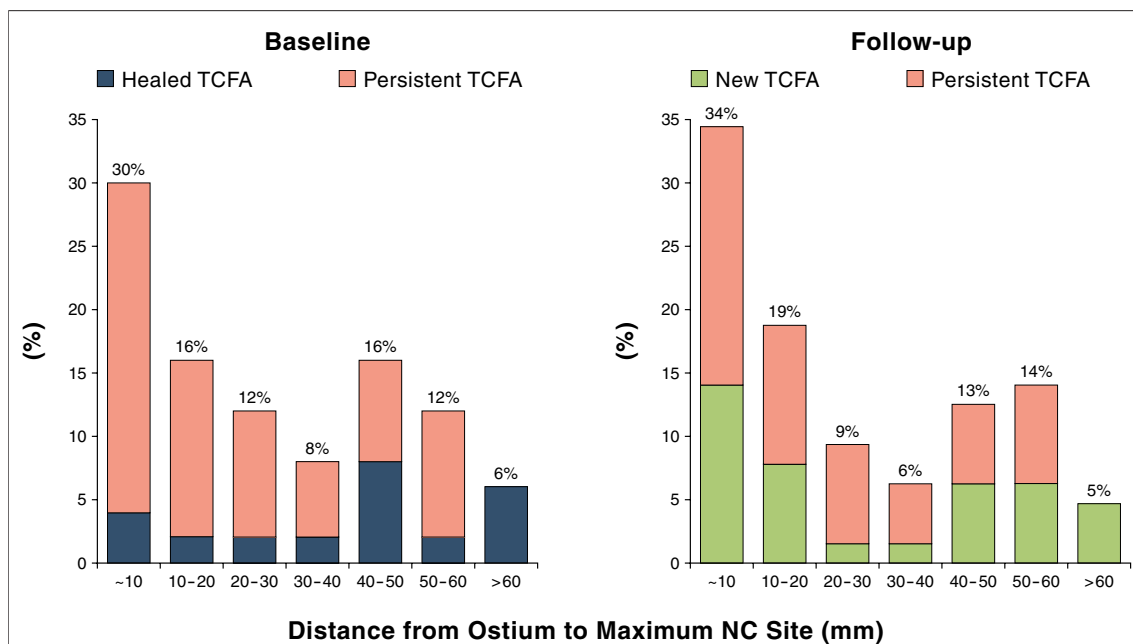
Figure 3. Longitudinal Distribution of TCFA at the Fibroatheroma Level at Baseline and Follow-Up

On the **left**, baseline TCFA are divided according to the response during follow-up: healing (defined as formation of a definable fibrous cap that isolated the NC from the lumen) or persisting. On the **right**, TCFA at follow-up are divided according to whether they are new TCFA (defined as disappearance of fibrous cap or increase of NC leading to more NC abutting to the lumen) or those that persisted from baseline. Overall, 46% of TCFA at baseline and 53% of TCFA at follow-up were in the proximal 20 mm of a coronary artery. Using the distance from the coronary ostium to the maximum NC site, TCFA that healed during follow-up tended toward being located more distally than TCFA that did not change. Abbreviations as in Figure 1.

that did not change or that became more unstable tended to be more proximally.

Characterization of the nonculprit lesion phenotype. In the current prospective study in patients with STEMI, 82% of secondary, nonculprit lesions were fibroatheromas, with half of these (41%) having a TCFA phenotype at baseline. The high rate of fibroatheromas are consistent with an earlier study by Asakura et al. (16), who reported that in 20 noninfarcted vessels, yellow, nondisrupted plaques as seen by angioscopy were present in most patients 1 month after a myocardial infarction (MI). By contrast, in the IVUS study by Kubo et al. (13) in patients mainly with stable ischemic heart disease, only 43% and 9% of secondary lesions had a ThCFA and TCFA phenotype at baseline, respectively. Thus, these data suggest that patients with STEMI compared with those without acute coronary syndromes are significantly more likely to have fibroatheromas and TCFAs at untreated, nonculprit lesion sites. These studies are also consistent with reports of simultaneous plaque ruptures in some patients with STEMI (8,17).

Other intravascular imaging studies have compared secondary lesions in stable versus unstable patients. Nakamura et al. (18) showed that TCFA were more common in ACS patients compared with stable patients (64.6% vs 35.7%, p = 0.006). Hong et al. (8) performed a 3-vessel grayscale IVUS study of 235 patients (122 acute MI, 113 stable angina); secondary plaque ruptures were present in 21 MI patients (17%) versus 6 stable patients (5%, p = 0.008). In a 3-vessel IVUS study, Hong et al. (19) reported a higher frequency of TCFA and plaque ruptures in secondary lesions in patients with ACS compared with stable angina (69% vs. 45%, and 8% vs. 4%, respectively, both p < 0.001). Using integrated backscatter IVUS (another radiofrequency IVUS technique), Ando et al. (20) showed a larger percent lipid area (p = 0.03) and a smaller percent fibrotic plaque area (p = 0.04) in nonculprit lesions in ACS patients compared with stable angina patients. Finally, Kubo et al. (21), using optical coherence tomography (OCT), reported that fibrous cap thickness (111 ± 65 vs. 181 ± 70 μm, p = 0.002) was significantly thinner and the frequency of OCT-derived TCFA (38% vs. 6%, p = 0.030) was significantly greater in acute MI than in stable angina.

Table 4. Baseline and Follow-Up Findings of Patients With Late Revascularization Events in Nonculprit Lesions

			Case #			
			1	2	3	4
Vessel			RCA	LAD	RCA	LM
Time from baseline, days			404	786	936	448
IVUS phenotype		Baseline	ThCFA	ThCFA	PIT	TCFA
		Follow-up	TCFA	TCFA	ThCFA	TCFA
Minimum lumen area site	Lumen CSA, mm^2	Baseline	6.9	3.4	7.5	5.4
		Follow-up	5.6	3.3	5.7	4.5
	Plaque burden, %	Baseline	68.2	58.1	59.3	71.3
		Follow-up	68.0	53.9	62.3	71.5
	% NC	Baseline	6.0	20.0	3.0	25.0
		Follow-up	11.0	26.0	23.0	40.0
Maximum NC site	Lumen CSA, mm^2	Baseline	9.0	3.4	9.8	5.36
		Follow-up	8.2	3.7	6.4	5.9
	Plaque burden, %	Baseline	60.7	58.1	44.4	71.3
		Follow-up	59.5	52.1	58.3	65.5
	%NC	Baseline	12.0	20.0	10.0	25.0
		Follow-up	33.0	36.0	24.0	43.0

LAD = left anterior descending; LM = left main coronary artery; RCA = right coronary artery; other abbreviations as in Tables 2 and 3.

Serial intravascular imaging assessment of nonculprit lesion phenotype. There have been few serial intravascular imaging studies assessing changes in lesion phenotype of unruptured, secondary plaques in stable or unstable patients (13,22–25). Using serial (baseline and follow-up) IVUS in patients with mostly stable ischemic heart disease, Kubo et al. (13) reported that most nonculprit TCFA stabilized or healed during 13 months of follow-up. By contrast, in the current study in patients with STEMI, nonculprit TCFA remained unchanged or became more unstable over time, while more stable lesions evolved into more unstable phenotypes. Of note, both of these studies were analyzed at the same core laboratory (CRF) using the same analytic techniques and definitions. A comparison of these 2 studies showing the difference between stable and unstable patients is shown in Figure 4.

The current study is also consistent with 2 small serial angioscopy studies. In 1 study in 48 patients with ACS and previous MI, the 12-month healing rate of nonculprit, ruptured plaques was only 30%
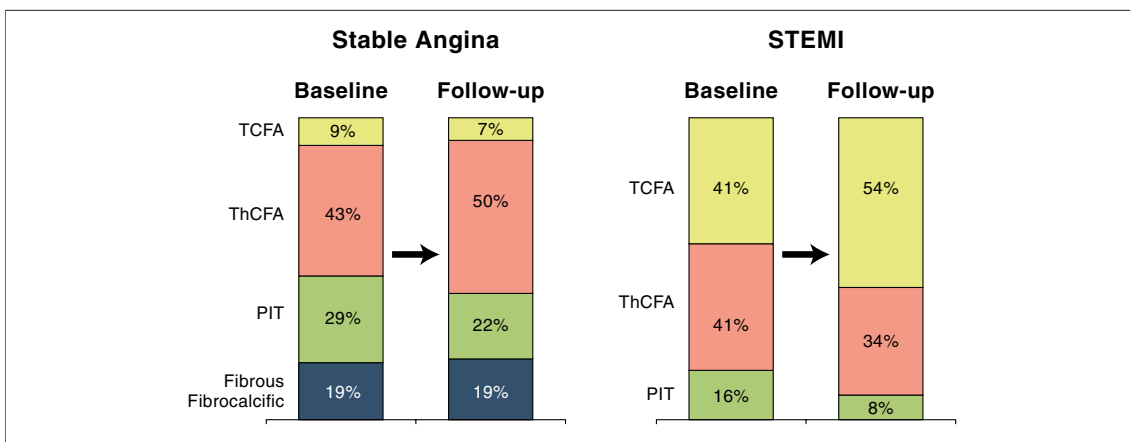

Figure 4. Comparison of 2 Serial IVUS Studies Reported From the Same Core Laboratory

Patients with stable angina are shown on the **left**. At baseline, only 20 nonculprit lesions (9%) were TCFA; during follow-up, 15 (75%) TCFA "healed," and 5 (25%) TCFA remained unchanged (13). Patients from the current analysis are shown on the **right**. TCFA increased from 41% at baseline to 54% at 13-month follow-up, with 32 (78%) remaining unchanged, 9 evolving into ThCFAs or fibrotic plaques, and 21 new TCFA developing from either PITs or ThCFAs. Abbreviations as in Figures 1 and 2.

(22). In the second study in 13 consecutive acute MI patients, the number of nonculprit yellow plaques did not change from post-reperfusion to 6-month follow-up (24).

TCFA location and "increase of fibrous cap." In the current study of patients with STEMI, approximately 50% of TCFA were in the proximal 20 mm of a coronary artery at baseline. Numerous pathological, angiographic, and imaging studies have shown a similar, proximal predisposition of TCFAs, acute occlusions, or plaque ruptures. In a human autopsy study, Cheruvu et al. (5) reported that 50% of TCFAs were present within the first 22 mm of the left anterior descending and left circumflex arteries and the first 31 mm of the right coronary artery. In another ex vivo study using histology, IVUS, and OCT, Kume et al. (26) reported that 70% of TCFAs clustered in the first 30 mm of a coronary artery. Wang et al. (27) analyzed 208 consecutive STEMI patients and found that angiographic occlusions tended to cluster within the proximal third of each coronary artery. In a 3-vessel grayscale IVUS study, Hong et al. (28) evaluated the axial location of plaque rupture in 392 patients; plaque ruptures occurred mainly in proximal segments of the left anterior descending coronary artery, the proximal half of the left circumflex, and the proximal and distal segments of right coronary artery. In a subsequent IVUS analysis, Hong et al. (20) also reported that 83% of TCFA were located mainly within 40 mm of the coronary ostium. The current study extends these findings by showing that proximal TCFA tended to progress to more unstable phenotypes, whereas distal TCFA did not.

Technical considerations. In the current study, IVUS phenotype evolution was assessed at 2 levels: lesion level and fibroatheroma level because a single lesion may contain more than 1 discrete fibroatheroma. If there was more than 1 fibroatheroma subtype within a given lesion, a TCFA took precedence over ThCFA; thus, for example, even if a lesion contained multiple ThCFAs at baseline, the evolution of only 1 ThCFA into a TCFA changed the overall lesion phenotype classification into a TCFA. Such heterogeneous changes at the fibroatheroma level increased the frequency of TCFA classification significantly, from 41% at baseline to 54% at 13-month follow-up at the lesion level.

Study limitations. Several limitations of the present study should be noted. Despite the fact that the HORIZONS-AMI is one of the largest IVUS multicenter trials, this substudy is of modest size and from a single center. Potential selection bias cannot be excluded. Most of the patients had IVUS in only 1 vessel, and none had 3-vessel imaging. The present results should therefore be considered exploratory and hypothesis generating. Details on lipid levels and corresponding pharmacotherapy are not available. IVUS generates only 1 image per every heart beat, thereby severely limiting coregistration and potentially causing misalignment between baseline and follow-up images. There were too few clinical events to permit a well-powered exploration of the relationship between recurrent events and plaque morphology as disclosed by IVUS. The anatomic locations and distributions of the lesions in this study vary from the typical distribution of culprit lesions as well as from the distribution of culprit lesions in the HORIZONS trial. As a result, lesions in this substudy may be subjected to different shear stress and other atherogenic factors that may influence progression compared with culprits There was no control group, and the number of new TCFA was too small to identify predictors of the transition from stable to vulnerable phenotype.

CONCLUSIONS

Untreated, nonculprit lesions in patients with STEMI are frequently fibroatheromas and typically become increasingly unstable during 13-month follow-up, with a decrease in MLA, increase in NC, and overall devolution to a TCFA morphology.

REFERENCES

1. Virmani R, Burke AP, Farb A, Kolodgie FD. Pathology of the vulnerable plaque. J Am Coll Cardiol 2006;47:C13–18.

2. Shah PK. Mechanisms of plaque vulnerability and rupture. J Am Coll Cardiol 2003;41:15S–22S.

3. Giroud D, Li JM, Urban P, Meier B, Rutishauer W. Relation of the site of acute myocardial infarction to the most severe coronary arterial stenosis at prior angiography. Am J Cardiol 1992;69:729–32.

4. Virmani R, Kolodgie FD, Burke AP, Farb A, Schwartz SM. Lessons from sudden coronary death: a comprehensive morphological classification scheme for atherosclerotic lesions. Arterioscler Thromb Vasc Biol 2000;20:1262–75.

5. Cheruvu PK, Finn AV, Gardner C, et al. Frequency and distribution of thin-cap fibroatheroma and ruptured plaques in human coronary arteries: a

pathologic study. J Am Coll Cardiol 2007;50:940–9.

6. Finn AV, Nakano M, Narula J, Kolodgie FD, Virmani R. Concept of vulnerable/unstable plaque. Arterioscler Thromb Vasc Biol 2010;30: 1282–92.

7. Kolodgie FD, Virmani R, Burke AP, et al. Pathologic assessment of the vulnerable human coronary plaque. Heart 2004;90:1385–91.

8. Hong MK, Mintz GS, Lee CW, et al. Comparison of coronary plaque rupture between stable angina and acute myocardial infarction. A three-vessel intravascular ultrasound study in 235 patients. Circulation 2004;110:928–33.

9. Nair A, Margolis P, Kuban BD, Vince DG. Automated coronary plaque characterization with intravascular ultrasound backscatter: ex vivo validation. EuroIntervention 2007;3:113–20.

10. Rodriguez-Granillo GA, García-García HM, McFadden EP, et al. In vivo intravascular ultrasound-derived thin-cap fibroatheroma detection using ultrasound radiofrequency data analysis. J Am Coll Cardiol 2005;46: 2038–42.

11. Nasu K, Tsuchikane E, Katoh O, et al. Accuracy of in vivo coronary plaque morphology assessment: a validation study of in vivo virtual histology compared with in vitro histopathology. J Am Coll Cardiol 2006;47:2405–12.

12. Stone GW, Maehara A, Lansky AJ, et al., The PROSPECT Investigators. A prospective natural-history study of coronary atherosclerosis. N Engl J Med 2011;364:226–35.

13. Kubo T, Maehara A, Mintz GS, et al. The dynamic nature of coronary artery lesion morphology assessed by serial virtual histology intravascular ultrasound tissue characterization. J Am Coll Cardiol 2010;55:1590–7.

14. Maehara A, Cristea E, Mintz GS, et al. Definitions and methodology for the grayscale and radiofrequency intravascular ultrasound and coronary angiographic analysis. J Am Coll Cardiol Img 2012;5:S1–9.

15. Lian KY, Zeger SL. Longitudinal data analysis using generalized linear models. Biometrika 1986;73:13–22.

16. Asakura M, Ueda Y, Yamaguchi O, et al. Extensive development of vulnerable plaques as a pan-coronary process in patients with myocardial infarction: an angioscopic study. J Am Coll Cardiol 2001;37:1284–8.

17. Goldstein JA, Demetriou D, Grines CL, Pica M, Shoukfeh M, O'Neill WW. Multiple complex coronary plaques in patients with acute myocardial infarction. N Engl J Med 2000; 343:915–22.

18. Nakamura T, Kubo N, Funayama H, Sugawara Y, Ako J, Momomura S. Plaque characteristics of the coronary segment proximal to the culprit lesion in stable and unstable patients. Clin Cardiol 2009;32:E9–12.

19. Hong MK, Mintz GS, Lee CW, et al. A three-vessel virtual histology intravascular ultrasound analysis of frequency and distribution of thin-cap fibroatheromas in patients with acute coronary syndrome or stable angina pectoris. Am J Cardiol 2008; 101:568–72.

20. Ando H, Amano T, Matsubara T, et al. Comparison of tissue characteristics between acute coronary syndrome and stable angina pectoris. An integrated backscatter intravascular ultrasound analysis of culprit and nonculprit lesions. Circ J 2011;75:383–90.

21. Kubo T, Imanishi T, Kashiwagi M, et al. Multiple coronary lesion instability in patients with acute myocardial infarction as determined by optical coherence tomography. Am J Cardiol 2010;105:318–22.

22. Takano M, Inami S, Ishibashi F, et al. Angioscopic follow-up study of coronary ruptured plaques in nonculprit lesions. J Am Coll Cardiol 2005;45: 652–8.

23. Hong MK, Mintz GS, Lee CW, et al. Serial intravascular ultrasound evidence of both plaque stabilization and lesion progression in patients with ruptured coronary plaques: effects of statin therapy on ruptured coronary plaque. Atherosclerosis 2007;191: 107–14.

24. Okada K, Ueda Y, Matsuo K, et al. Frequency and healing of nonculprit coronary artery plaque disruptions in patients with acute myocardial infarction. Am J Cardiol 2011;107:1426–9.

25. Hong YJ, Jeong MH, Choi YH, et al. Impact of baseline plaque components on plaque progression in nonintervened coronary segments in patients with angina pectoris on rosuvastatin 10 mg/day. Am J Cardiol 2010;106: 1241–7.

26. Kume T, Okura H, Yamada R, et al. Frequency and spatial distribution of thin-cap fibroatheroma assessed by 3-vessel intravascular ultrasound and optical coherence tomography: an ex vivo validation and an initial in vivo feasibility study. Circ J 2009;73: 1086–91.

27. Wang JC, Normand SL, Mauri L Kuntz RE. Coronary artery spatial distribution of acute myocardial infarction occlusions. Circulation 2004; 110:278–84.

28. Hong MK, Mintz GS, Lee CW, et al. The site of plaque rupture in native coronary arteries: a three-vessel intravascular ultrasound analysis. J Am Coll Cardiol 2005;46:261–5.